such as **2** are expected to be the *most* sensitive of aromatics to ring current effects, for normal biphenyl-type aromatics interaction between the rings will be more readily observed through UV spectra than nuclear magnetic resonance data.

Experimental Section

^{1}H NMR spectra were determined in $CDCl_3$ on a Perkin-Elmer R32 (90 MHz) spectrometer and are reported in parts per million downfield from tetramethylsilane as internal standard. UV spectra were determined in cyclohexane on a Cary 17 spectrophotometer. Mass spectra were determined on a Hitachi Perkin-Elmer RMU-7 (high-resolution) or Finnigan 3300 (low-resolution) mass spectrometer at 70 eV. Microanalyses were performed by this department and by Canadian Microanalytical services Ltd. All evaporations were carried out under reduced pressure on a rotary evaporator at ca. 40 °C. Extracts were dried with anhydrous sodium sulfate.

Bi(2,2′-*trans*-10b,10c-dimethyl-10b,10c-dihydropyrenyl) (2). A solution of *n*-butyllithium (0.2 mmol in hexane, 0.1 mL) was added under N_2 to a stirred solution of 2-bromo-*trans*-10b,10c-dimethyl-10b,10c-dihydropyrene (**5**)[8] (50 mg, 0.16 mmol) in dry ether (2 mL) in a flamed flask. After 5 min this solution was added under N_2 to a slurry of TlBr (0.08 g, 0.3 mmol) in benzene (2 mL) and ether (2 mL). The mixture was then heated under reflux with stirring for 4 h. It was then cooled, poured into water, and extracted with dichloromethane. The extract was washed, dried, and evaporated and the residue was chromatographed over silica gel. Pentane eluted first the green dimethyldihydropyrene **4**, ca. 10 mg, and then the purple bipyrene **2**, 13 mg (35% yield), as very dark greenish black crystals from methanol that formed purple solutions; mp ca. 195–199 °C dec; ^{1}H NMR δ 9.46 (s, 4 H, H-1,3), 8.8–8.5 (m, 14 H, other ArH), −3.68 and −3.77 (s, 6 H each, CH_3); MS, $M^{+\cdot}$ at *m/e* 462 (24%), 447 (M − CH_3, 38), 432(M − $2CH_3$, 26), 417 (M − $3CH_3$ 100), 402 (M − $4CH_3$, 55) plus many doubly charged ions; UV λ_{max} (log ϵ_{max}) 577 nm (4.20), 544 (sh, 4.13), 480 (sh, 3.80) 436 (3.83), 400 (4.12), 368 (4.72), 345 (4.42), 332 (sh, 4.35). Anal. Calcd for $C_{36}H_{30}$: C, 93.46; H, 6.54; mol wt., 462.23. Found: C, 92.91; H, 6.06; mol wt, 462.24 (MS). When anhydrous $CoCl_2$ (0.8 g) was used as oxidant (reflux, 4 h) from bromide **5** (800 mg), there was obtained bipyrene **2** (150 mg, 25% yield), identical with the above sample.

***trans*-10b,10c-Dimethyl-2-phenyl-10b,10c-dihydropyrene (3).** A solution of phenyllithium (3.2 mmol in hexane 1.8 mL) was added to a stirred slurry of CuBr (0.23 g 1.6 mmol) in dry ether (5 mL) at 0 °C under N_2. After 30 min the solution was allowed to warm to ca. 20 °C and a solution of the bromodihydropyrene **5**[8] (100 mg, 3.2 mmol) in dry ether (5 mL) was added. The mixture was kept at ca. 20 °C for 8 days. Nitrobenzene (0.2 mL) was then added and stirring maintained for ca. 15 min, after which the mixture was poured into water and extracted with dichloromethane. The extract was washed, dried, and evaporated, and the residue was chromatographed over silica gel using pentane as eluant. Eluted first was some parent dihydropyrene **4** (10–20 mg) followed by the purple biphenyl **3**, which on recrystallization from methanol–water gave yellow-green needles: 16 mg (16% yield); mp 118–119 °C, which on dissolution form purple solutions; ^{1}H NMR δ 8.91 (s, 2 H, H-1,3), 8.8–8.5 (m, 6 H, H-4,5,6,8,9,10), 8.3–7.9 (m, 3 H, H-7,2′,6′), 7.8–7.4 (m, 3 H, H-3′,4′,5′), −4.00, −4.03 (s, 3 H each, CH_3); MS, $M^{+\cdot}$ at *m/e* 308 (30%), 293 (M − CH_3, 97), 278 (M − $2CH_3$, 100); UV λ_{max} (log ϵ_{max}) 648 nm (2.51), 620 (sh, 2.35), 493 (4.18), 390 (4.52), 366 (4.41), 348 (5.15), 330 (4.56), 279 (4.08), 246 (4.11). Anal. Calcd for $C_{22}H_{20}$: C, 93.46; H, 6.54; mol wt, 308.16. Found: C, 93.25; H, 6.75; mol wt, 308.17 (MS).

Coupling Using Bis(triphenylphosphino)nickel(II) Chloride as a Precursor to Ni^0. Preparation of 2 and 3. Bis(triphenylphosphino)nickel(II) chloride[20] (105 mg, 0.16 mmol), triphenylphosphine (84.2 mg, 0.32 mmol), and zinc dust (10.6 mg, 0.16 mmol) were slurried in dry O_2-free DMF (5 mL) in a flamed flask under N_2. The mixture was then heated to 50 °C with stirring for 1 h, and then the bromopyrene **5**[8] (50 mg, 0.16 mmol) in DMF (2 mL) was added. After 24 h at 50 °C the reaction mixture was cooled, poured into dilute aqueous HCl, and extracted with ether. The extract was washed, dried, and evaporated. Chromatography on silica gel using pentane as eluant gave first dimethyldihydropyrene **4** (~10 mg, 27%), then the symmetrical dipyrene **2** (~ 15 mg, 41%), and finally the unsymmetrical biphenyl **3** (~8 mg, 16%) all contaminated with triphenylphosphine. The latter could only be removed by HPLC using a reverse-phase column with methanol as eluant. The biphenyl's **2** and **3** showed retention times identical with those of the samples previously described.

Registry No. 2, 92720-01-9; **3**, 92720-02-0; **4**, 956-84-3; **5**, 71807-14-2; PhLi, 591-51-5; $(Ph_3P)_2NiCl_2$, 14264-16-5.

(20) Yamamoto, K. *Bull. Chem. Soc. Jpn.* **1954**, *27*, 501–505.

Oxygenation Patterns for Iron(II) Porphyrins. Peroxo and Ferryl ($Fe^{IV}O$) Intermediates Detected by ^{1}H Nuclear Magnetic Resonance Spectroscopy during the Oxygenation of (Tetramesitylporphyrin)iron(II)

Alan L. Balch,* Yee-Wai Chan, Ru-Jen Cheng, Gerd N. La Mar, Lechoslaw Latos-Grazynski, and Mark W. Renner

Contribution from the Department of Chemistry, University of California, Davis, California 95616. *Received March 20, 1984*

Abstract: The reaction between unligated (tetramesitylporphyrin)iron(II) ($TMPFe^{II}$) and dioxygen in a toluene solution has been examined by ^{1}H NMR spectroscopy. At −70 °C, $TMPFe^{II}$ reacts with O_2 to yield $TMPFe^{III}OOFe^{III}TMP$ that has spectroscopic properties similar to those of other peroxo-bridged complexes. On warming, $TMPFe^{III}OOFe^{III}TMP$ decomposes to yield a second intermediate (identified as $TMPFe^{IV}O$) and $TMPFe^{III}OH$, the final, stable product. $TMPFe^{III}OOFe^{III}TMP$ reacts with *N*-methylimidazole (*N*-MeIm) to produce (*N*-MeIm)$TMPFeO_2$ and (*N*-MeIm)$_2TMPFe^{II}$. The former has been independently prepared from (*N*-MeIm)$_2TMPFe^{II}$ and dioxygen at −50 °C. $TMPFe^{IV}O$ reacts with *N*-MeIm to form (*N*-MeIm)$TMPFe^{IV}O$ that has been identified by comparison with other $Fe^{IV}O$ complexes. $TMPFe^{IV}O$ reacts with triphenylphosphine at −50 °C to yield triphenylphosphine oxide while $TMPFe^{III}OOFe^{III}TMP$ is unreactive toward triphenylphosphine under these conditions. $TMPFe^{II}$ is a catalyst for the oxidation of triphenylphosphine by dioxygen. ^{1}H NMR spectra and resonance assignments for each species are described.

Introduction

The autoxidation of iron(II) porphyrins, PFe (P is a porphyrin dianion), in the absence of other axial ligands generally leads to the formation of an oxo-bridged species as shown in eq 1.[1] This

$$4PFe^{II} + O_2 \rightarrow 2PFe^{III}\text{–}O\text{–}Fe^{III}P \quad (1)$$

transformation represents a simple case of dioxygen activation by a transition metal system, and it is one where it is possible to

0002-7863/84/1506-7779$01.50/0

study the reaction mechanism by detecting reaction intermediates, particularly at low temperatures where they have increased lifetimes. At some stage the reaction path must involve what is a fundamental aspect of all dioxygen activation: cleavage of the oxygen–oxygen bond. Equation 2 reproduces a path that has been suggested for this reaction. Here, O–O bond rupture leads to the formation of a ferryl ($Fe^{IV}O$) complex.

$$PFe^{II} + O_2 \longrightarrow PFeO_2 \xrightarrow{PFe^{II}} \underset{A}{PFe^{III}\text{-}O\text{-}O\text{-}Fe^{III}P} \longrightarrow \underset{B}{2PFe^{IV}O} \xrightarrow{2PFe^{II}} 2PFe^{III}O\,Fe^{III}P \quad (2)$$

In previous work, it has been possible to detect the first two intermediates in this path. Synthetic iron(II) porphyrins, such as (*meso*-tetraphenylporphyrin)iron(II) ($TPPFe^{II}$) and (octaethylporphyrin)iron(II) ($OEPFe^{II}$) are oxygenated in an inert solvent (toluene or dichloromethane) at low temperatures to produce peroxo-bridged complexes $PFe^{III}OOFe^{III}P$.[2-4] These can be observed by ^1H NMR and electronic spectra and are stable in solution indefinitely at −70 °C. Upon warming, they are converted into $PFe^{III}OFe^{III}P$ with the liberation of dioxygen. No intermediates have been detected during this process. The peroxo-bridged species resembles the oxo-bridged complexes[5,6] in that they are an antiferromagnetically coupled system.

By using sterically hindered iron porphyrins such as **1–4**, it is possible to inhibit the formation of the oxo- and peroxo-bridged species, $PF^{III}OFe^{III}P$ and $PFe^{III}OOFe^{III}P$. Under these conditions,

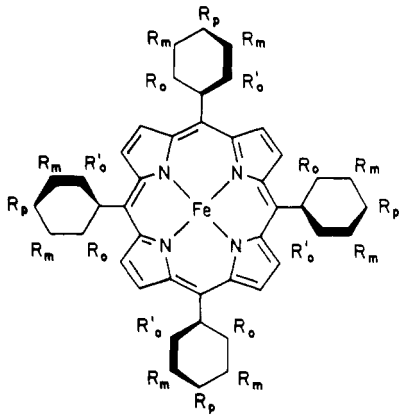

1. R'_o = *t*-BuC(=O)NH–; $R_o = R_m = R_p = H$
2. $R'_o = R_o = R_p = OCH_3$; $R_m = H$
3. $R'_o = R_o = R_p = OCH_2CH_3$; $R_m = H$
4. $R_m = R_p = OCH_3$; $R'_o = R_o = H$
5. $R'_o = R_o = R_p = CH_3$; $R_m = H$, TMPFe

it is possible to observe the first intermediate in eq 2. This substance, $PFeO_2$, has been detected in solution by ^1H NMR and electronic spectroscopy.[7] It is a diamagnetic species that is stable in solution at low temperatures. Related compounds with unhindered porphyrins have been detected by infrared spectroscopy using matrix isolation techniques.[8]

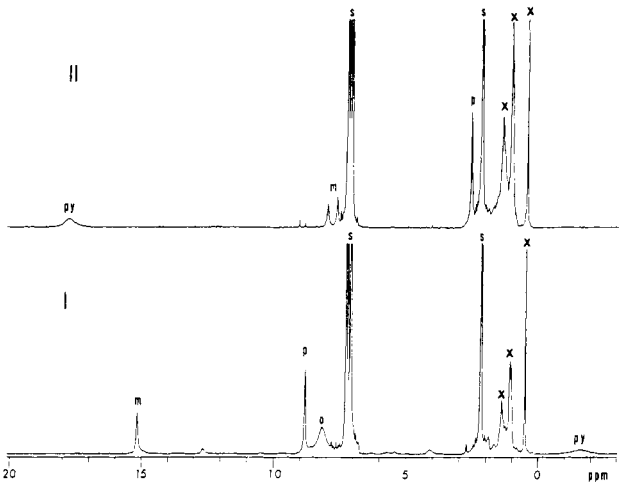

Figure 1. The 360-MHz ^1H NMR spectra of toluene-d_8 solutions at −70 °C of I, $TMPFe^{II}$, II, $TMPFe^{II} + O_2$ (1 atm), the species present in II is intermediate A, TMPFeOOFeTMP. Resonances are identified by the following symbols: py, pyrrole protons; m, meta-mesityl protons; o, ortho-mesityl methyl protons; p, para-mesityl methyl protons; S, residual undeuterated solvent; X, impurities in the solvent.

While intermerdiates are not normally detected during the decomposition of $PFe^{III}OOFe^{III}P$, it is possible to stablize the product of O–O bond rupture by having an amine present. Thus, $PFe^{III}OOFe^{III}P$ reacts at −70 °C with amines (B = *N*-methylimidazole (*N*-MeIm), pyridine, or piperidine) to form six-coordinate $BPFe^{IV}O$ according to eq 3.[4,9] This is irreversible. The

$$PFe^{III}OOFe^{III}P + 2B \rightarrow BPFe^{IV}O \quad (3)$$

product has a triplet ground state with a magnetic moment of 2.9 μ_B. Its characteristic ^1H NMR spectra show very small hyperfine shifts that strictly obey the Curie law. Like $PFe^{III}OOFe^{III}P$, $BPFe^{IV}O$ is indefinitely stable at −80 °C but decomposes fairly rapidly at −30 °C. The physical properties (^1H NMR spectra,[4] electronic spectra,[9] magnetic moment,[9] Mössbauer spectra,[10] and EXAFS spectra[11]) of $BPFe^{IV}O$ closely resemble those of the enzyme intermediate, compound II of horseradish peroxidase.[12] Quantitative transfer of the oxygen atom from iron to triphenylphosphine has been observed.[13]

Since the metal–metal separation is about 1 Å greater in a peroxo-bridged compound than it is in an oxo-bridged species, it should be possible to construct steric constraints so that peroxo-bridge formation is allowed while oxo-bridge formation is prohibited. If this could be arranged, then conversion of $PFe^{III}OOFe^{III}P$ directly to $PFe^{IV}O$ might be directly observed. Tetramesitylporphyrin[14] offers just this opportunity. We have previously demonstrated that this porphyrin does not form an oxo-bridged compound.[15] Rather, both procedures that usually form PFeOFeP, reaction of hydroxide with PFeCl or oxygenation of PFe^{II}, result in the synthesis of $TMPFe^{III}OH$.[15,16] Here we describe the results of our observations on the oxygenation path for $TMPFe^{II}$, **5**.

(1) For a review, see: (a) James, B. R. In "The Porphrins"; Dolphin, D., Ed.; Academic Press: New York, 1978; Vol. 5, pp 205–302. (b) Collman, J. P. *Acc. Chem. Res.* **1977**, *10*, 265–272. (c) Collman, J. P.; Halpert, T. R.; Suslick, K. S. In "Metal Ion Activation of Dioxygen"; Spiro, T., Ed.; Wiley: New York, 1980; pp 1–72.
(2) Chin, D.-H.; Del Gaudio, J.; La Mar, G. N.; Balch, A. L. *J. Am. Chem. Soc.* **1977**, *99*, 5486–5488.
(3) Chin, D.-H.; La Mar, G. N.; Balch, A. L. *J. Am. Chem. Soc.* **1980**, *102*, 4344–4350.
(4) La Mar, G. N.; de Ropp, J. S.; Latos-Grazynski, L.; Balch, A. L.; Johnson, R. B.; Smith, K. M.; Parish, D. W.; Cheng, R.-J. *J. Am. Chem. Soc.* **1983**, *105*, 782–787.
(5) Murray, K. S. *Coord. Chem. Rev.* **1974**, *12*, 1–35.
(6) La Mar, G. N.; Eaton, G. R.; Holm, R. H.; Walker, F. A. *J. Am. Chem. Soc.* **1973**, *95*, 63–75.
(7) Latos-Grazynski, L.; Cheng, R.-J.; La Mar, G. N.; Balch, A. L. *J. Am. Chem. Soc.* **1982**, *104*, 5992–6000.
(8) Nakamoto, K.; Watanabe, T.; Ama, T.; Urn, M. W. *J. Am. Chem. Soc.* **1982**, *104*, 3744–3745.
(9) Chin, D. H.; Balch, A. L.; La Mar, G. N. *J. Am. Chem. Soc.* **1980**, *102*, 1446–1448.
(10) Simmonneaux, G.; Scholz, W. F.; Reed, C. A.; Lang, G. *Biochim. Biophys. Acta* **1982**, *716*, 1–7.
(11) Penner-Hahn, J. E.; McMurry, T. J.; Renner, M.; Latos-Grazynski, L.; Eble, K. S.; Davis, I. M.; Balch, A. L.; Groves, J. T.; Dawson, J. H.; Hodgson, K. O. *J. Biol. Chem.* **1983**, *258*, 12761–12764.
(12) Dunford, H. B.; Stillman, J. S. *Coord. Chem. Rev.* **1976**, *19*, 187–251.
(13) Chin, D. H.; La Mar, G. N.; Balch, A. L. *J. Am. Chem. Soc.* **1980**, *102*, 5945–5947.
(14) Badger, G. M.; Jones, R. A.; Laslett, R. L. *Aust. J. Chem.* **1964**, *17*, 1028–1035.
(15) Cheng, R.-J.; Latos-Grazynski, L.; Balch, A. L. *Inorg. Chem.* **1982**, *21*, 2412–2418.
(16) Groves, J. T.; Haushalter, R. C.; Nakamura, M.; Nemo, T. E.; Evans, B. J. *J. Am. Chem. Soc.* **1981**, *103*, 2884–2886.

Table I. ^{1}H NMR Data

compd	temp, °C	chemical shifts,[a] ppm			
		pyrrole	phenyl substituents		
			ortho	meta	para
$TMPFe^{II}$	−79	−1.7	8.1	15.1	8.7
$TPPFe^{II}$	−70	−2.4	(26.2)[c]	14.5	(14.8)[c]
$[TMPFe^{III}O]_2$	−70	17.7	...	7.9, 7.5	2.5
$[TPPFe^{III}O]_2$	−70	16.4	(7.8, ...)[c]	7.6, ...	(7.6)[c]
$TMPFe^{IV}O$	−70	8.4	3.3, ...	6.4, 6.0	2.6
$TMPFe^{III}OH$[b]	−70	116.4	...	17.7, 15.6	4.5
$TMPFe^{III}Cl$[b]	−70	120.0	...	20.4, 17.7	5.1
$TMPFe^{II}(N\text{-MeIm})_2$	−77	8.8	2.2	...	2.5
$TMPFe^{II}(N\text{-MeIm})_2$	25	8.7	2.1	7.2	2.4
$TMPFe(N\text{-MeIm})O_2$	−77	8.37	...	...	...
$(N\text{-MeIm})TMPFe^{IV}O$	−60	...	3.6, ...	7.5, ...	2.74
$(N\text{-MeIm})TMPFe^{IV}O$	−30	4.6	3.2, 1.6	7.4, ...	2.67
$(N\text{-MeIm})TPPFe^{IV}O$	−80	5.05	(9.2, ...)[c]	7.9, ...	(7.9)[c]

[a] In toluene-d_8 solution with tetramethylsilane as reference. [b] Data from ref 15. [c] Phenyl protons

Results

^{1}H NMR Characterization of Thermally Stable Iron Complexes. Since the ^{1}H NMR spectra of iron porphyrins offer a sensitive technique for distinguishing between the various spin/oxidation/ligation states of the metal,[18] this has been used as the principal method for following the oxygenation reactions. ^{1}H NMR spectral parameters for stable compounds as well as reaction intermediates are collected into Table I. The physical properties of $TMPFe^{III}Cl$ and $TMPFe^{III}OH$ have been described earlier.[15] Reduction of either of these in toluene-d_8 solution with either aqueous sodium dithionite[19,20] or zinc amalgam[7] produces red $TMPFe^{II}$. Both reduction techniques with either starting material yield identical spectral results. The ^{1}H NMR spectrum (shown in trace I of Figure 1) and the electronic spectrum of $TMPFe^{II}$ are typical of those of other planar, unligated iron(II) porphyrins with $S = 1$ ground states.[7,20] Corresponding data for $TPPFe^{II}$ are given in Table I for comparison. Characteristically, the pyrrole resonance shows Curie temperature dependence but has an extrapolated position at infinitely high temperature of 20.1 ppm that is far from the corresponding diamagnetic position.[20] Addition of an excess of *N*-MeIm to $TMPFe^{II}$ produces diamagnetic $TMPFe^{II}(N\text{-MeIm})_2$. Again, the ^{1}H NMR parameters are consistent with those of other six-coordinate, low-spin iron(II) porphyrins.[20]

Oxygenation of $TMPFe^{II}$ and Formation of Intermediate A ($TMPFe^{III}OOFe^{III}TMP$). Introduction of dioxygen into a toluene-d_8 solution of $TMPFe^{II}$ at −70 °C results in the spectral changes which are seen by comparing trace I and trace II of Figure 1. The resonances of $TMPFe^{II}$ have been replaced with those of an intermediate, A, which can confidently be identified as $TMPFe^{III}OOFe^{III}TMP$. The identity of the pyrrole resonances has been confirmed by specific deuteration of the pyrrole positions and the meta-phenyl resonances have been assigned by their position and relative intensity. The presence of two meta-phenyl resonances indicates that the environments on either side of the porphyrin plane differ in A as they should in a bridged porphyrin dimer. The chemical shifts of the protons in A are similar to those of other previously characterized peroxo-bridged iron porphyrins like $TPPFe^{III}OOFe^{III}TPP$ (see Table I).[3] Moreover, the chemical shift of the pyrrole resonance in A shows distinct non-Curie behavior. It moves from 17.7 ppm at −70 °C to 19.0 ppm at −30 °C. The direction and magnitude of this shift are consistent with corresponding data on other peroxo-bridged iron porphyrins.[2,3]

As with other peroxo-bridged iron(III) porphyrins, the formation A from $TMPFe^{II}$ and dioxygen is irreversible. A sample of A has been subject to three freeze (liquid nitrogen)–pump–thaw (−80 °C bath) cycles. The ^{1}H NMR spectrum of this sample was unchanged in the process. In particular, there was no evidence for the presence of $TMPFe^{II}$ in the sample.

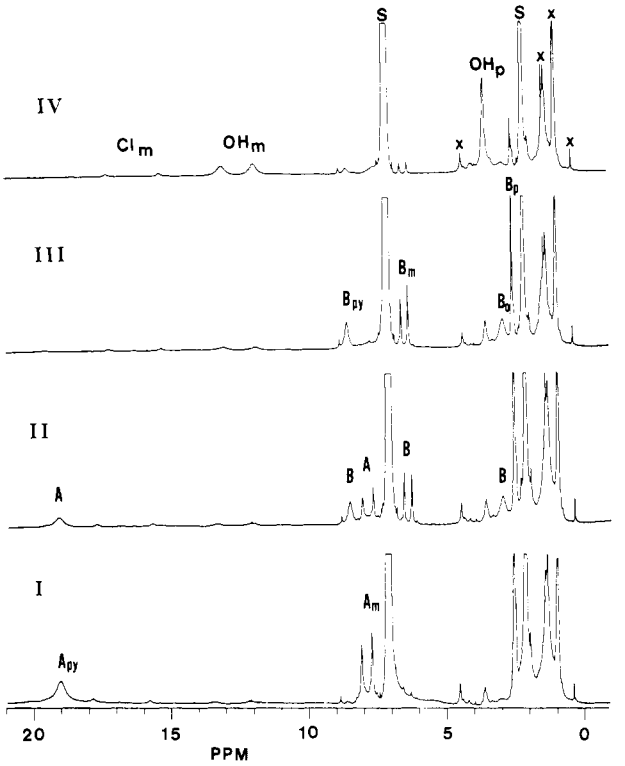

Figure 2. 360-MHz ^{1}H NMR spectra showing the thermal decomposition of ~4 mM TMPFeOOFeTMP in toluene-d_8 solution under 1 atm of dioxygen: trace I, intermediate A TMPFeOOFeTMP, at −30 °C; trace II, sample from I kept at −30 °C for 1 h; trace III, sample from trace II kept at −20 °C. Resonances due to individual species are denoted by capital letters: A, TMPFeOOFeTMP; B, TMPFeO; OH, TMPFeOH; Cl, TMPFeCl from incomplete reduction; S, solvent; X, impurities. Subscripts refer to resonance assignments as follows: py, pyrrole; m, meta-H; o, ortho-CH_3; p, para-CH_3.

Formation of Intermediate B during the Thermal Decomposition of Intermediate A, TMPFeOOFeTMP. Intermediate A is unstable, as the data in Figure 2 show. In trace I we see the spectrum of A that was prepared at −70 °C and warmed to −30 °C. The sample contains some $TMPFe^{III}Cl$ (peaks labeled Cl) that is present as a result of incomplete reduction in the initial generation of $TMPFe^{II}$. The presence of this amount of $TMPFe^{III}Cl$ makes a useful intensity standard. In addition, some $TMPFe^{III}OH$ (peaks labeled OH), the final decomposition product, is present. (Peaks due to the pyrrole protons of $TMPFe^{III}Cl$ and $TMPFe^{III}OH$, which are observed at 99.5 and 96.9 ppm, are offscale on the figure and

(17) Adler, A. D.; Longo, F. R.; Kampus, F.; Kim, J. *J. Inorg. Nucl. Chem.* **1970**, *32*, 2443–2445.
(18) La Mar, G. N.; Walker, F. A. In "The Porphyrins"; Dolphin, D., Ed.; Academic Press: New York, 1979; Vol. 4, pp 61–157.
(19) Brault, D.; Rougee, M. *Biochemistry* **1974**, *13*, 4591–4597.
(20) Goff, H.; La Mar, G. N.; Reed, C. A. *J. Am. Chem. Soc.* **1977**, *99*, 3641–3646.

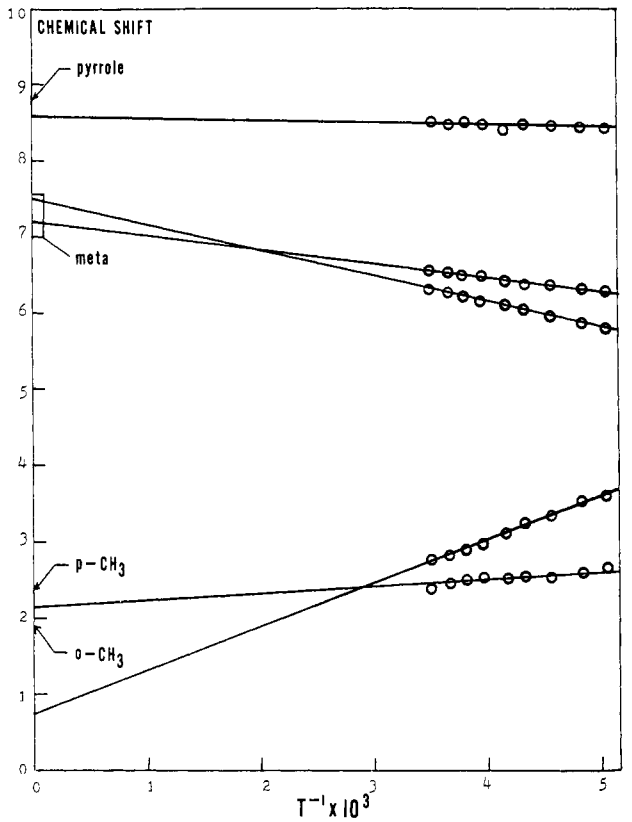

Figure 3. A Curie plot of the chemical shifts of intermediate B, $TMPFe^{IV}O$.

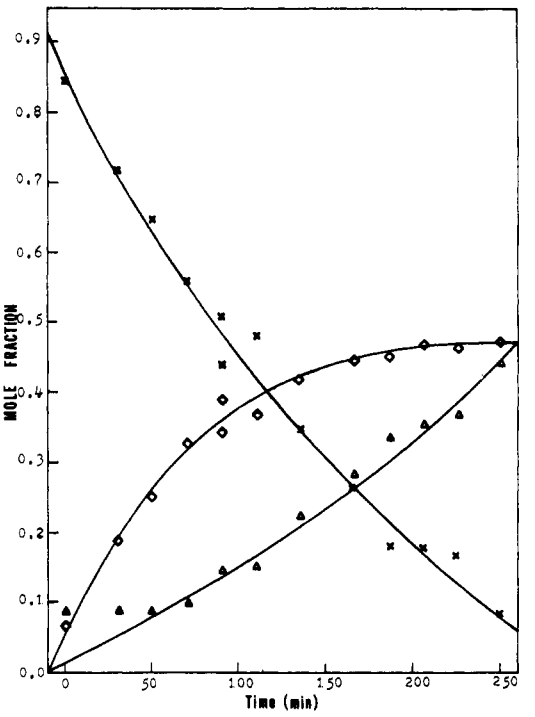

Figure 4. The mole fractions of intermediate A, TMPFeOOFeTMP, intermediate B, $TMPFe^{IV}O$ and TMPFeOH, during thermal decomposition of A in toluene solution at −30 °C: crosses, TMPFeOOFeTMP; squares, $TMPFe^{IV}O$; triangles, TMPFeOH.

are not shown.) On standing at −30 °C, the peaks due to A decrease in intensity as shown in trace II (obtained after 1 h at −30 °C) and trace III (obtained after 2 h at −20 °C). The rate of decay of the resonances of A can be hastened by warming to higher temperature. As A decomposes, two new species, an unstable intermediate, B, and the final stable product $TMPFe^{III}OH$, form. The transformation of A into B and then to $TMPFe^{III}OH$ is an irreversible process. Once B is formed we have not observed its conversion back to A. Likewise the conversion of $TMPFe^{III}OH$ directly to B or A has not been observed. The overall yield involved in the transformation of A to $TMPFe^{III}OH$ based on integration of the data in Figure 2 is 95 ± 5%. No other iron porphyrin is detected as a product of the reaction.

The resonances of B are clearly seen in traces II and III. The pyrrole resonance of B has been identified by specific deuteration. As with A, a doublet for the meta-phenyl protons has been identified by integration. The methyl resonances have also been identified by their area. The narrowest of these three lines has been assigned to the para-methyl group. The presence of two meta-proton resonances indicates that the axial ligation differs a either side of the porphyrin plane. A Curie plot of the chemical shifts for intermediate B is shown in Figure 3. As can be seen, the shifts are very small but are linear. Two lines of evidence indicate that intermediate B is a paramagnetic species. Firstly, all resonances of B are paramagnetically relaxed and the observed trend in line widths for the functional groups (ortho-CH_3 > pyrrole > meta-H> para-CH_3) is the same as the relative r^{-6} (r is the metal–group distance) values. This is indicative of metal-centered dipolar relaxation that is found for most iron porphyrins.[18] Secondly, although the hyperfine shifts are small, all signals follow the Curie law with appropriate intercepts near the known diamagnetic position for each functional group. This is inconsistent with an equilibrating mixture and indicates that B exists as a unique, well-defined paramagnetic species. The small hyperfine shifts are similar to those observed for the $BPFe^{IV}O$ for which a triplet state has been established from magnetic susceptibility studies that yield a magnetic moment per iron of 2.9 μ_B with strict Curie behavior.[9] Consequently we propose a triplet state for B.

Intermediate B eventually decays into $TMPFe^{III}OH$ as the sole, stable iron porphyrin product of the oxygenation reaction. This can be seen in trace IV of Figure 2. This trace has obtained after the sample was warmed from −30 °C to room temperature and then cooled back to −30 °C. The concentration of $TMPFe^{III}OH$ has increased, and neither of the intermediates A or B remain.

The variation of concentrations of A, B, and $TMPFe^{III}OH$ as a function of time (over a limited time period) can be seen in Figure 4. . The loss of A is accompanied by the increase in concentrations of first B and then of the final product $TMPFe^{III}OH$. As the plot shows, intermediate B is never the sole iron porphyrin present in solution; it is always accompanied by either A or $TMPFe^{III}OH$ or both. This has limited our ability to gain certain information about this intermediate. In particular, we have had difficulties in measuring the magnetic susceptibility of B.

The rate of decay of A follows first-order kinetics as shown in Figure 5. At −30 °C the rate constant for decay of A is 0.008 (1) min^{-1}. This is somewhat slower than the rate of decay of $TmTPFe^{III}OOFe^{III}TmTP$ (TmTP is *meso*-tetra-*m*-tolylporphyrin dianion) that at −32 °C has a rate constant of 0.035 (3) min^{-1}.[3]

Reactions of Intermediates A and B with Bases. Treatment of a toluene solution of A with *N*-MeIm at −70 °C yields the ^1H NMR spectrum shown in Figure 6, inset B, which shows the region of the pyrrole resonances. These are the resonances that are normally the most sensitive to structural differences. Two pyrrole resonances are clearly detected. The low-field pyrrole resonance (as well as the methyl resonances) are identified as arising from $TMPFe^{II}(N\text{-MeIm})_2$ that has been prepared independently from $TMPFe^{II}$ and excess *N*-MeIm. The spectrum of $TMPFe^{II}(N\text{-MeIm})_2$ is shown in the lower trace in Figure 6, and the pyrrole region is expanded in inset A. The second pyrrole resonance in inset B is due to a thermally unstable species whose resonance intensity decreases upon warming. This is seen by comparing insets B and C of Figure 6. An identical pyrrole resonance can be generated by adding dioxygen to a sample of $TMPFe^{II}(N\text{-MeIm})_2$ at low temperature. Inset D of Figure 6 shows the result. Notice that the intensity of this second resonance is quite low in both insets C and D. We identify the species responsible for the higher field pyrrole resonance as the dioxygen complex (*N*-MeIm)$TMPFeO_2$.

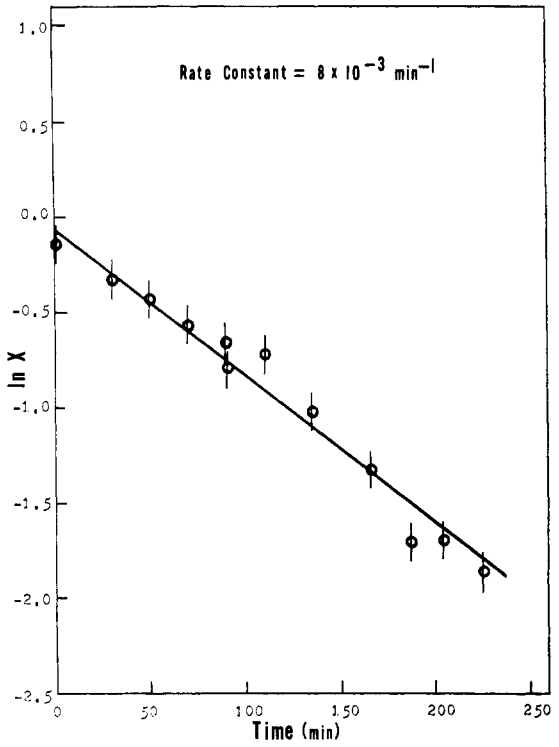

Figure 5. Plot showing first-order decay of intermediate A, TMPFeOOFeTMP, in toluene-d_8 at −30 °C.

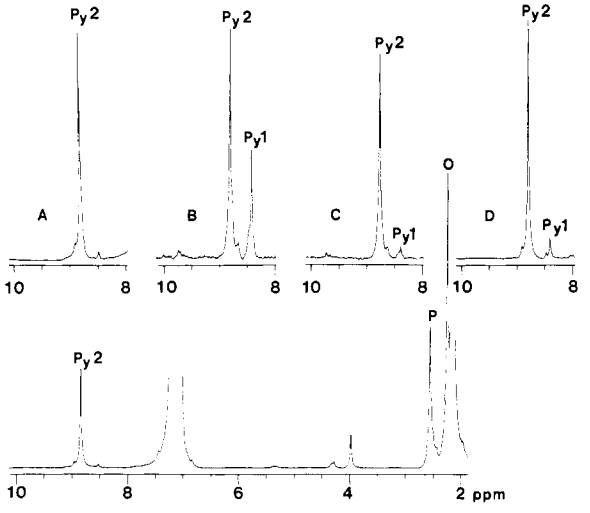

Figure 6. 360-MHz ^{1}H NMR spectra of toluene solutions at −70 °C: bottom, (N-MeIm)$_2$TMPFe^{II}; inset A, expanded pyrrole region for (N-MeIm)$_2$TMPFe^{II}; inset B, pyrrole region for intermediate A (1 mM), TMPFeOOFeTMP, and excess (4 mM) N-MeIm; inset C, same as B after warming to −50 °C; inset D, (N-MeIm)$_2$TMPFe^{II} + O_2 at −70 °C. Resonance assignments: Py^2, pyrrole porotons of (N-MeIm)$_2$TMPFe^{II}; Py, pyrrole protons of (N-MeIm)TMPFeO$_2$; o, ortho-mesityl methyl protons; p, para-mesityl methyl protons.

A similar complex, (N-MeIm)TPPFeO$_2$, has been observed at low temperature.[21] From the intensity of the pyrrole resonances, it is clear that at −50 °C the equilibrium given in eq 4 favors the

$$\text{TMPFe}^{II}(N\text{-MeIm})_2 + O_2 \rightleftharpoons (N\text{-MeIm})\text{TMPFeO}_2 + N\text{-MeIm} \quad (4)$$

$$\text{TMPFeOOFeTMP} + 3N\text{-MeIm} \rightarrow \text{TMPFe}^{II}(N\text{-MeIm})_2 + (N\text{-MeIm})\text{TMPFeO}_2 \quad (5)$$

reactants under the conditions of the experiment. Having

(21) Weschler, C. J.; Anderson, D. L.; Basolo, F. *J. Am. Chem. Soc.* **1975**, *97*, 6707–6713.

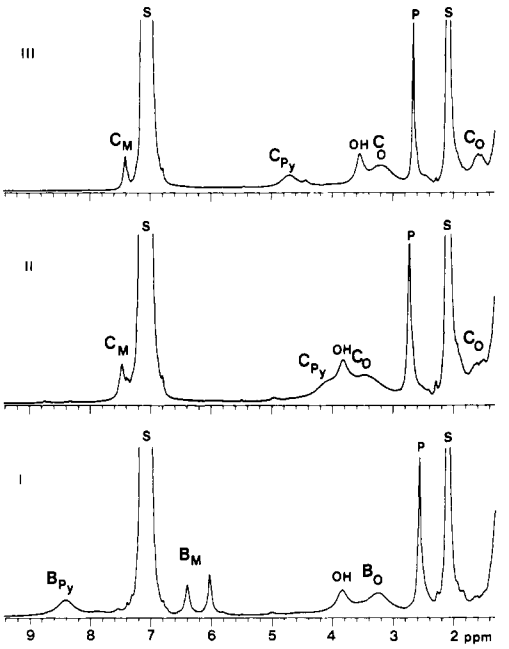

Figure 7. 360-MHz ^{1}H NMR spectra showing the effect of adding N-methylimidazole to intermediate B, TMPFe^{IV}O: trace I, a toluene solution of B (~4 mM) at −60 °C; trace II, the same solution after the addition of 50 μL (63 mM solution) of N-methylimidazole at −60 °C, (N-MeIm)TMPFe^{IV}O is present; trace III, the same solution at −30 °C. Resonance assignments; Py, pyrrole; m, meta-mesityl; o, ortho-mesityl methyl; p, para-mesityl methyl; s, solvent; OH, para-mesityl methyl of TMPFeOH.

identified both products, we can now specify that the reaction between A and N-MeIm proceeds according to eq 5 with the second product (N-MeIm)TMPFeO$_2$ undergoing subsequent substitution of the dioxygen with N-MeIm.

The results of the addition of N-MeIm to intermediate B can be ascertained by examining the data in Figure 7. Comparison of traces I and II show that B is converted into a new species, C. (The TMPFe^{III}OH, which is present, is unaffected by the addition of N-MeIm, and the TMPFeOOFeTMP present reacts via eq 5 as previously described.) The resonances of the new intermediate C are labeled according to their assignment of Figure 7, trace II. Again, the pyrrole resonance has been unambiguously identified by specific deuterium and the other resonances identified by their relative areas, line widths, and their extrapolated positions at infintely high temperature. A second meta-phenyl resonance is probably hidden under the large solvent resonance at 7 ppm. Trace III shows the corresponding spectrum obtained at −30 °C where some of the resonances are shifted into positions that make them more readily observable. The temperature dependence of the chemical shifts of the protons follows the Curie law. The relative data are shown in Figure 8. The chemical shifts observed for the protons in C and the Curie behavior, with the pyrrole resonance extrapolating to 9 ppm (its diamagnetic position), are similar to the properties previously described for (N-MeIm)TPPFe^{IV}O. This similarity allows us to identify C as (N-MeIm)TMPFe^{IV}O.

The reactions of intermediate A and B with triphenylphosphine and triphenylarsine have also been examined. At −70 °C, A is unreactive toward an excess of triphenylarsine or triphenylphosphine. At −50 °C, a dioxygen-free solution of B reacts with triphenylphosphine to yield triphenylphosphine oxide. It also reacts under similar conditions with triphenylarsine to yield triphenylarsine oxide. These latter reactions have been monitored by ^{1}H NMR spectroscopy that allows us to not only detect the loss of B but also the formation of triphenylphosphine oxide through the observation of a characteristic multiplet at 7.70 ppm and of triphenylarsine whose characteristic multiplet occurs at 7.66 ppm. The selectivity of the triphenylphosphine reaction with a mixture of A and B is demonstrated in Figure 9. Trace I of Figure 9 shows the ^{1}H NMR spectrum of a mixture of intermediate A, inter-

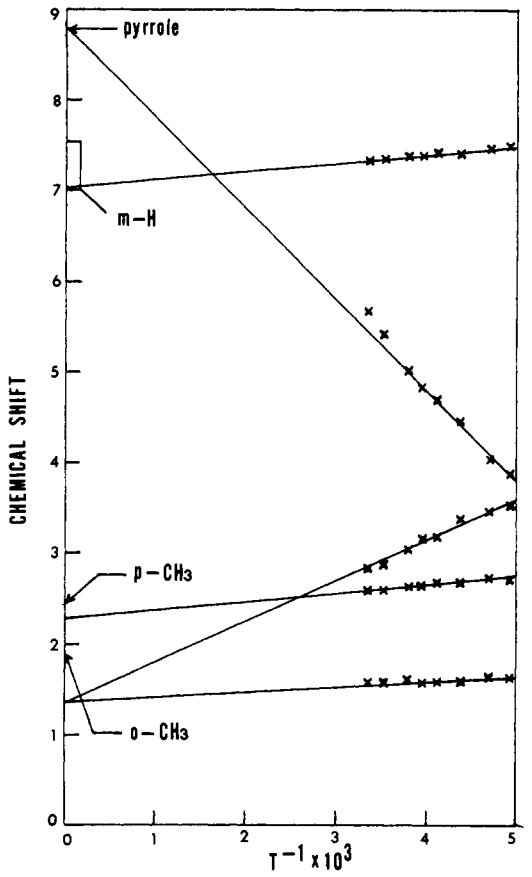

Figure 8. A Curie plot for intermediate C, (*N*-MeIm)TMPFe^{IV}O.

mediate B, and TMPFeOH. Upon treatment with triphenylphosphine at −70 °C, the spectrum shown in trace II is obtained. All resonances due to B have been lost. New resonances due to triphenylphosphine and triphenylphosphine oxide are observed. Resonances due to A remain unaffected.

As with other iron porphyrins, TMPFe^{II} is a catalyst for the reaction between triphenylphosphine and dioxygen to form triphenylphosphine oxide. At 25 °C, under 1 atm of dioxygen, about 40 turnovers are possible before the catalyst becomes inactive. Analysis of the inactivated catalyst shows that TMPFe^{III}OH, which like other iron(III) porphyrins is inactive toward triphenylphosphine, is present.

Discussion

The oxygenation pattern observed for TMPFe^{II} differs in several significant ways from those of other iron(II) porphyrins that we have previously examined. The initial formation of the peroxo-bridged species TMPFeOOFeTMP (intermediate A) is typical of most unhindered synthetic iron porphyrins including TPPFe^{II} and OEPFe^{II}.[3,4] Unlike the sterically hindered porphyrins **1–4**, there is not evidence with TMPFe^{II} for the formation of the diamagnetic dioxygen complex ($PFeO_2$). Oxygenation of these hindered iron(II) porphyrins and of TMPFe^{II} has been carried out under similar conditions so that it is likely that, if present, $TMPFeO_2$ would have been detected. However, we have not made exhaustive efforts to prepare and detect $TMPFeO_2$. The formation of the peroxo-bridged intermediate in this case is not prevented by the presence of the ortho methyl groups.

The thermal decomposition of TMPFe^{III}OOFe^{III}TMP produces a detectable intermediate (B) whose existence precedes the formation of the final iron(III) product. Thus oxygenation of TMPFe^{II} is unlike any other system examined so far. B represents an important newly detected intermediate in iron porphyrin oxygenation. We identify this intermediate, B, as the five-coordinate ferryl complex TMPFe^{IV}O for the following reasons.

We have argued previously that the rate-determining step in the thermal decomposition of other peroxo-bridged iron porphyrins

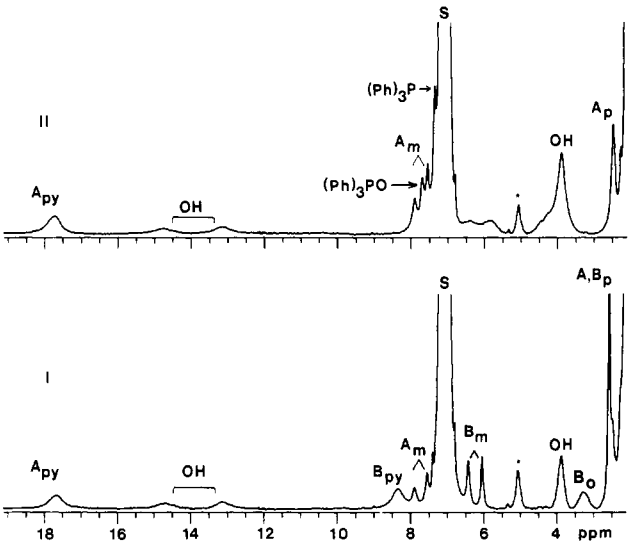

Figure 9. 360-MHz ^{1}H NMR spectra showing the effect of triphenylphosphine on a mixture of TMPFeOOFeTMP and TMPFe^{IV}O Trace I, the spectrum of the intermediates before triphenylphosphine addition; Trace II, the spectrum of the same mixture after triphenylphosphine addition. Resonance assignments: A, intermediate A; B, intermediate B; py, pyrrole protons; m, meta-mesityl protons; o, ortho-mesityl methyl; p, para-mesityl methyl; OH, resonances of TMPFeOH.

is cleavage of the O–O bond to produce PFe^{IV}O. In all other cases, PFe^{IV}O has remained undetectable because of its high reactivity. Our proposed mechanism of decomposition of other peroxo-bridged iron(III) porphyrins is shown in eq 6–9. In this scheme, in a

$$PFe^{III}\text{–O–O–}Fe^{III}P \rightarrow 2PFe^{IV}O \quad (6)$$

$$PFe^{IV}O + PFe^{III}\text{–O–O–}Fe^{III}P \rightarrow PFe^{III}O\text{–}Fe^{III}P + O_2FeP \quad (7)$$

$$O_2FeP \rightleftharpoons O_2 + PFe^{II} \quad (8)$$

$$PFe^{IV}O + PFe^{II} \rightarrow PFe^{III}\text{–O–}Fe^{III}P \quad (9)$$

toluene solution at low temperature, PFe^{IV}O is lost through attack on other iron porphyrins (eq 7 and 9). However, with the degree of steric protection available to TMPFe^{IV}O, this should not be possible. TMPFe^{III}–O–Fe^{III}TMP does not exist, as we have shown earlier. Consequently, the ferryl group in TMPFe^{IV}O is so buried that it cannot attack another hindered iron site. As a result TMPFe^{IV}O, once formed, is forced to undergo decay via another reaction path. This path leads to TMPFe^{III}OH.

Further evidence for the formulation of B as TMPFe^{IV}O comes from its reaction with *N*-MeIm that yields C. C can confidently be identified as (*N*-MeIm)TMPFe^{IV}O from the similarity of its ^{1}H NMR spectrum of that of the previously characterized (*N*-MeIm)TPPFe^{IV}O. Consequently, conversion of B to C is simply an addition of *N*-MeIm into the vacant coordination site in B, TMPFe^{IV}O. The difference between the ^{1}H NMR spectra of B and C suggests that differences exist in their electronic structure. Although both show unusually small hyperfine shifts for paramagnetic species, the direction of the pyrrole and meta-phenyl proton shifts are reversed in the two species.

The observation of two meta-phenyl proton resonances for B is in accord with the proposed structure which has an oxo ligand on one side of the porphyrin plane and no ligand on the opposite side.

The reactivity toward oxygen atom acceptors is also accord with a ferryl formulation for B. Previous work[13] has shown that in general PFeOOFeP itself is unreactive toward triphenylphosphine at −70 °C; however, on warming, it does oxidize triphenylphosphine to the oxide. The rate-determining step in this process has been shown to be the same as the rate of O–O bond clevage in PFeOOFeP. Consequently, we have proposed that it is PFe^{IV}O which is the actual oxidant. Additionally, (*N*-MeIm)TmTPFe^{IV}O has been shown to react with triphenylphosphine to form tri-

phenylphosphine oxide quantitatively and to react with triphenylarsine to form triphenylarsine oxide. The observation that $TMPFe^{III}OOFe^{III}TMP$ is unreactive toward triphenylphosphine at −70 °C is in accord with earlier observations of other peroxo-bridged compounds. The fact that intermediate B does react with triphenylphosphine provides additional support for the presence of the ferryl group in B.

The reaction of TMPFeOOFeTMP with *N*-MeIm is unusual in that this reaction is customarily a route to $(N\text{-MeIm})PFe^{IV}O$. With TMPFeOOFeTMP, however, an Fe–O rather than an O–O bond is broken so that $(N\text{-MeIm})TMPFeO_2$ and $TMPFe^{II}(N\text{-MeIm})_2$ are the initial products. While this is a unique example of reaction for *N*-MeIm, we have previously observed other cases of Fe–O bond breaking in the reactions of bases with peroxo-bridged complexes. For example, we have seen that methyl isocyanide reacts with $TPPFe^{III}OOFe^{III}TPP$ according to eq 10.[22]

$$TPPFe^{III}OOFe^{III}TPP + 3MeNC \rightarrow (MeNC)TPPFeO_2 + TPPFe^{II}(MeNC)_2 \quad (10)$$

It should be noted that another oxo complex of TMPFe is known. Treatment of $TMPFe^{III}X$ with *m*-chloroperoxybenzoic acid yields a transient species that has been formulated at [TMPFeO]X, a ferryl ($Fe^{IV}O$) complex with a porphyrin π-radical ligand.[16] This species has ^1H NMR spectral characteristics that are clearly distinct from those of any of the species reported here. It is, of course, one oxidation state higher than $TMPFe^{IV}O$ or $(N\text{-MeIm})TMPFe^{IV}O$ and dioxygen must not be a sufficiently strong oxidant to transform $TMPFe^{IV}O$ into $[TMPFe^{IV}O]^+$. In fact, the interrelation and interconversion of these species remains under study in our laboratory.

While the present work is particularly satisfying because it has allowed the direct observation of $TMPFe^{IV}O$, a previously suspected species involved in iron porphyrin oxygenation, some aspects of the chemistry remain to be resolved. At present we have no information that allows for the prediction of whether a peroxo-bridged iron porphyrin will react via Fe–O or O–O bond breaking. Both have been observed in reactions with amines. The reducing agent responsible for the conversion of $TMPFe^{IV}O$ into $TMPFe^{III}OH$ has not been identified nor has the source of the protons in the product been found. A quantitative assessment of the magnetic susceptibility and hence the spin state of $TMPFe^{IV}O$ is lacking.

(22) Latos-Grazynski, L.; Balch, A. L., unpublished results.

Experimental Section

Materials. $TMPH_2$ was prepared by a modification[23] of the previous route.[14] Iron was inserted to form $TMPFe^{III}Cl$ by a standard route.[24] $TMPFe^{III}OH$ was prepared as described earlier.[15] 1,2,3,4,5,6,7,8-Octadeuterio-*meso*-tetramesitylporphyrin was obtained from pyrrole-d_5 prepared by a standard method.[25]

Preparation of Samples for Spectroscopic Study. Unligated $TMPFe^{II}$ was prepared by reduction of $TMPFe^{III}Cl$ in toluene solution with aqueous sodium dithionite solution or zinc amalgam in a Vacuum Atmospheres controlled-atmosphere box under purified argon. Typically 1 mg of $TMPFe^{II}$ and 5 mg of sodium dithionite were dissolved in a mixture of 0.5 mL of dichloromethane and several drops of water. The solutions were shaken to mix the two layers. After reduction was complete, as noted by a color change from green-brown to red, the two phases were allowed to separate and the aqueous layer was removed by a pipet. The dichloromethane layer was washed with a sample of dioxygen-free water to remove inorganic salts. The dichloromethane was evaporated under vacuum and the sample of $TMPFe^{II}$ was dried for 12 h under continuous vacuum pumping. The $TMPFe^{II}$ was then dissolved in deoxygenated toluene-d_8 and transferred to an NMR tube that was subsequently sealed with a septum cap. The sample was then removed from the controlled atmosphere box and cooled to −80 °C. Dry dioxygen and other chemicals were added to the cold sample with a syringe.

Spectroscopic Measurements. ^1H NMR spectra were recorded at 360 MHz on a Nicolet NT-360 spectrometer operating in the quadrature mode. Peak positions (in ppm) were referenced against tetramethylsilane. Typical spectra required 300–2000 transients collected over a 10-kHz band width with a 10-μs 90° pulse.

Acknowledgment. We thank the National Institutes of Health (GM-26226) for support. L.L.-G was on leave from the Institute of Chemistry, University of Wroclaw, Wroclaw, Poland.

(23) Cheng, R.-J.; Ph. D. Thesis, University of California, Davis, 1982.
(24) Adler, A. D.; Longo, F. R.; Finarelli, J. D.; Goldmacher, J.; Assour, J.; Korsakoff, L. *J. Org. Chem.* **1967**, *32*, 476–483.
(25) Fajar, J.; Borg, D. C.; Forman, A.; Felton, R. H.; Vegh, L.; Dolphin, D. *Ann. N.Y. Acad. Sci.* **1973**, *206*, 349–362.

Simultaneous Double N-Inversion Pathway

M. Kaftory* and I. Agmon

Contribution from the Department of Chemistry, Technion—Israel Institute of Technology, 32000 Haifa, Israel. *Received February 21, 1984*

Abstract: The pathway for simultaneous double N-inversion has been derived from geometric data given by crystal-structure determinations of various compounds containing the 1,2,4-triazolidinedione ring. Bond lengths and angles in this fragment are functions of the degree of flattening at the two mutually bonded N atoms. Two parameters were used to define the flattening at the N atoms: the displacement of the N–N bond (Δ) from the plane described by the four C atoms bonded to those two N atoms and the average of the valence angles at the N atoms (α_{av}). Bond lengths and angles are linearly related to α_{av} and logarithmically to Δ. Extrapolation of the bond lengths and angles according to their dependence on the degree of planarity provides the fragment's geometry at the transition state of the inversion. The results also show pronounced effect of the different substituents at the triazolidinedione ring. Statistical treatment suggests that only three independent factors concerning three molecular centers dominate the changes in the geometry of the molecular fragment during the inversion.

The subject of atomic inversion has been extensively studied since the early work of Meisenheimer and co-workers,[1] who suggested that an inversion process was responsible for the inability of trivalent nitrogen to sustain optical activity. In an atomic inversion process, a reversal of configuration results, although no bonds are broken and no other chemical reactant is required. Inversion at nitrogen is perhaps the most thoroughly studied process in this field. The inversion process, in general, and its energy barrier, in particular, have other implications apart from interest in the mechanism. Flattening at nitrogen occurs in electron loss processes as well as in nitrogen inversion. Thus, it is believed[2,3]

(1) Meisenheimer, J.; Angerman, C.; Finn, O.; Vieweg, E. *Ber.* **1924**, *57*, 1744–1759.

0002-7863/84/1506-7785$01.50/0